ARMY RESEARCH LABORATORY

Metallurgical Examination of Failed Spiral Bevel Gear P196, Part No. 145D6302

Marc S. Pepi

ARL-TR-1432 AUGUST 1997

The findings in this report are not to be construed as an official Department of the Army position unless so designated by other authorized documents.

Citation of manufacturer's or trade names does not constitute an official endorsement or approval of the use thereof.

Destroy this report when it is no longer needed. Do not return it to the originator.

Army Research Laboratory
Aberdeen Proving Ground, MD 21005-5066

ARL-TR-1432 August 1997

Metallurgical Examination of Failed Spiral Bevel Gear P196, Part No. 145D6302

Marc S. Pepi
Weapons & Materials Research Directorate

Abstract

A failed spiral bevel gear was examined by the U.S. Army Research Laboratory (ARL), Weapons and Materials Research Directorate, after the primary contractor (Boeing Helicopters Co.) performed the initial investigation. The gear was fabricated from X-2M steel. Light optical microscopy of the failed gear section revealed characteristics consistent with a fatigue failure. The fracture origin was characterized by a darkened, half-moon-shaped region. Energy-dispersive spectroscopy of the darkened region revealed the presence of sodium, evidence that the crack was open to the black oxide finish process. The pre-existing crack was oriented perpendicular to the direction of grinding, indicating the possibility of a grinding crack. Metallography confirmed that the pre-existing crack was a grinding burn, since evidence of rehardening and retempering was observed. Contributory to crack propagation was the presence of carbide networks within the carburized case. Metallographic examination, combined with microhardness testing, revealed a deeper than acceptable case in the damping ring groove region (origin location). It was later learned that this region was mistakenly subject to a double carburization during processing. Although the morphology of the origin was featureless, fractographic examination of a secondary fracture (most likely an additional grinding crack) did reveal an intergranular "rock candy" morphology. This was evidence that the crack propagated along the carbide network within the carburized case. It was concluded that the crack had formed during the grinding process and had propagated along the carbide network until final fast fracture.

TABLE OF CONTENTS

INTENTIONALLY LEFT BLANK

LIST OF FIGURES

LIST OF TABLES

INTENTIONALLY LEFT BLANK

METALLURGICAL EXAMINATION OF FAILED SPIRAL BEVEL GEAR P196, PART NO. 145D6302

1. BACKGROUND

A spiral bevel transmission gear (see Figure 1, taken from the Boeing report) from a CH-47D Army cargo helicopter failed during a training flight at Fort Meade, Maryland, leading to an immediate landing. Inspection of the Number 2 engine transmission revealed that an eight-tooth segment (of a 35-tooth gear) had fractured and penetrated the transmission housing. The failed component (Part No. 145D6302) was fabricated from Vasco X-2M steel and carburized to a required case hardness of 59 to 64 hardness Rockwell "C" (HRC). The failed component was originally examined by Boeing Helicopters (refer to Boeing Report [Materials Engineering Laboratory Report {MELR}] No. 93-105, dated 15 December 1995) [1], and subsequently shipped to the U.S. Army Research Laboratory (ARL), Weapons and Materials Research Directorate, for analysis. The broken part was subject to visual examination/light optical microscopy, chemical analysis, metallography, hardness testing/case depth measurement, X-ray diffraction, scanning electron microscopy (SEM) and energy-dispersive spectroscopy (EDS).

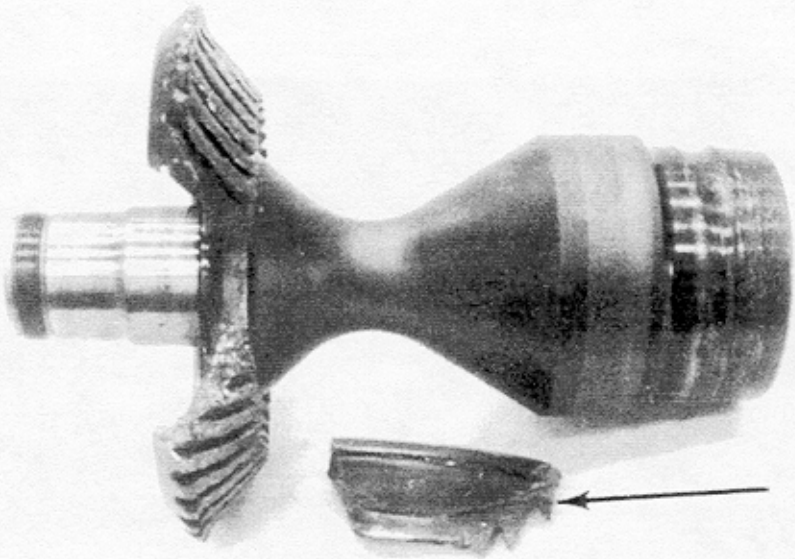

Figure 1. Optical Macrograph of the Failed Spiral Bevel Gear and the Fractured Eight-tooth Segment (denoted by the arrow). (The photo was reproduced from the Boeing report and reduced 70%.)

2. MATERIAL

Vasco X-2M was developed by Teledyne-Vasco of Latrobe, Pennsylvania, as a carburizing grade steel with good hot hardness for gear and shaft applications [2]. It has essentially the same chemical composition as H12 hot work die steel, with the exception of a lower carbon content. The X-2M variation has a further reduced carbon content than the X-2 predecessor. This alloy provides an excellent combination of strength, toughness, and fatigue strength.

3. VISUAL EXAMINATION/LIGHT OPTICAL MICROSCOPY

Visual examination and light optical microscopy of the fracture surfaces revealed characteristics consistent with a fatigue failure, including smoothness of fracture and beach marks (see Figure 2). The beach marks and radial lines on the fracture surface revealed that the origin was located in the damping ring groove portion of the gear at a darkened half-moon-shaped defect (see Figure 3). This region was located at the intersection of the 30° taper and the 7.125-inch diameter. The defect was oriented perpendicular to the direction of grinding, suggesting the possibility of a grinding crack. Further visual examination of the remaining component revealed small grinding cracks in the same area as the fracture origin.

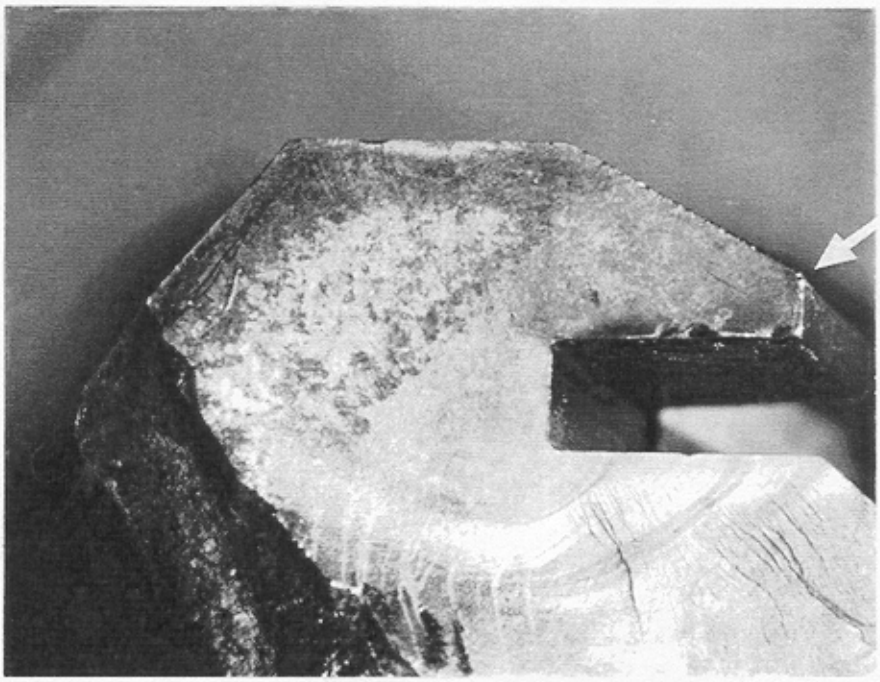

Figure 2. Optical Micrograph of the Primary Fracture Surface Showing Evidence of Fatigue (beach marks). (Arrow denotes fracture origin; magnification 7.5x.)

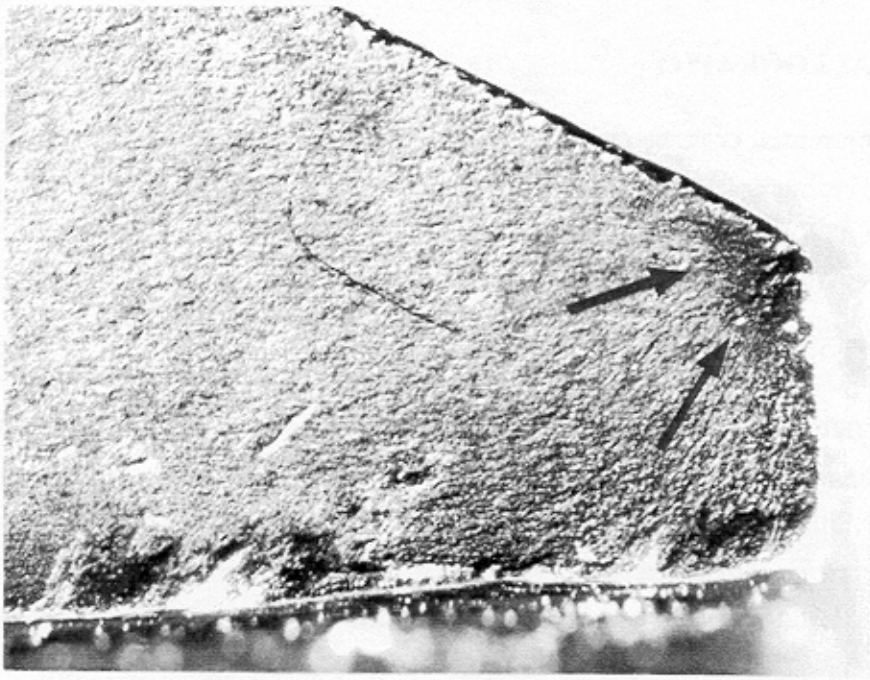

Figure 3. Magnified View of the Processing Defect Located at the Origin. (The grinding crack is denoted by arrows; magnification 40x.)

4. CHEMICAL ANALYSIS

The elemental composition of the X-2M steel was analyzed for conformance to the governing specification (Boeing Material Specification [BMS] 7-223C). The carbon content was determined by infrared detection combustion, while the sulfur was determined by automatic titration combustion. The weight percent of the remaining elements was determined through direct current plasma emission spectroscopy. The molybdenum content was slightly lower than specified; however, the remaining elements conformed to the governing specification. Table 1 lists the results of this analysis.

Table 1

Chemical Analysis
Weight Percent

	C	Si	Mn	S	P	W	Cr	V	Mo	Fe
Gear	0.15	0.86	0.28	<0.001	<0.004	1.33	5.17	0.42	1.25	*Rem.
Specification (BMS 7-223C)	0.13-0.16	0.80-1.10	0.20-0.40	0.010 max.	0.015 max.	1.20-1.50	4.75-5.25	0.40-0.50	1.30-1.50	Rem.

*Rem = remainder

5. METALLOGRAPHY

A circumferential cross section was taken through the origin to confirm that the pre-existing defect was a grinding crack. The sample was metallographically prepared and etched with Vilella's reagent (5 ml hydrochloric acid, 1 gram picric acid, and 100 ml ethanol). The sample showed evidence of rehardening (white region) and retempering (dark region) as shown in Figure 4. This pre-existing crack was oriented perpendicular to the direction of grinding, consistent with a grinding crack. Figure 5 is a montage showing the as-polished appearance of the fracture origin and several grinding cracks running parallel to the fracture plane. Figure 6 shows the same area after application of Vilella's reagent. Note that each grinding crack is contained within the grinding burn. Other grinding burns and grinding cracks were also noted adjacent to the fracture origin (see Figure 7). This burn was 0.43 inch away from the fracture origin. In addition, metallography revealed what appeared to be continuous carbide networks (CCNs) in the region of the gear that contained the origin (see Figure 8).

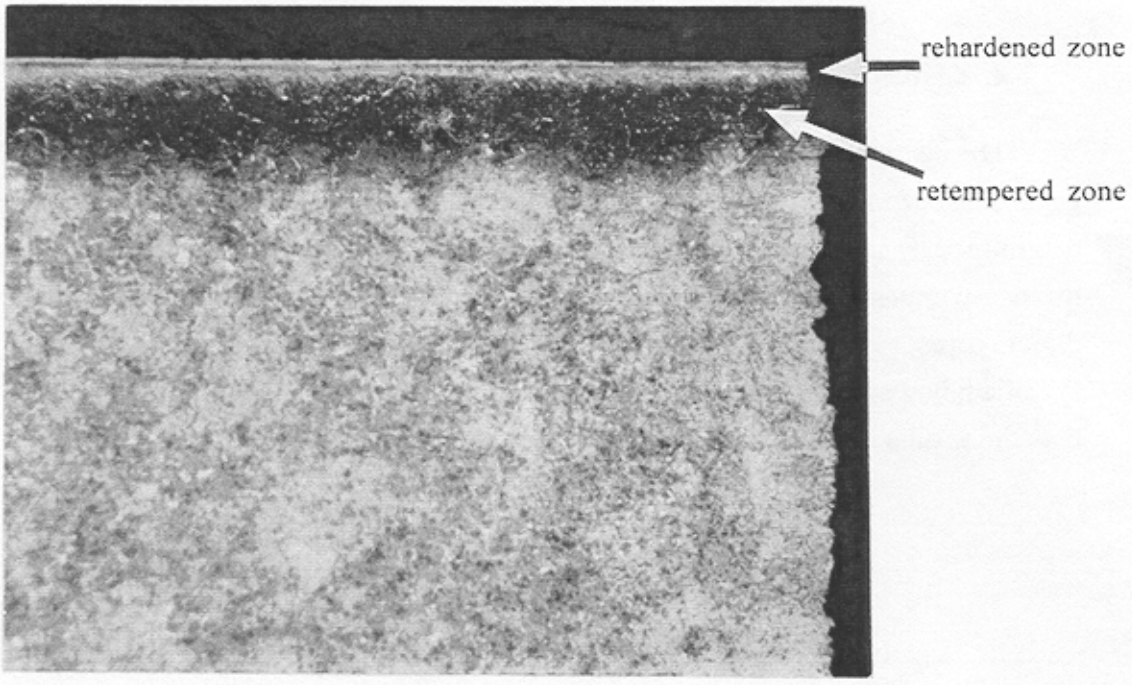

Figure 4. Metallographic Section Through the Origin. (Note the rehardened white layer and the retempered darkened layer caused by the grinding burn; Vilella's reagent; magnification 200x.)

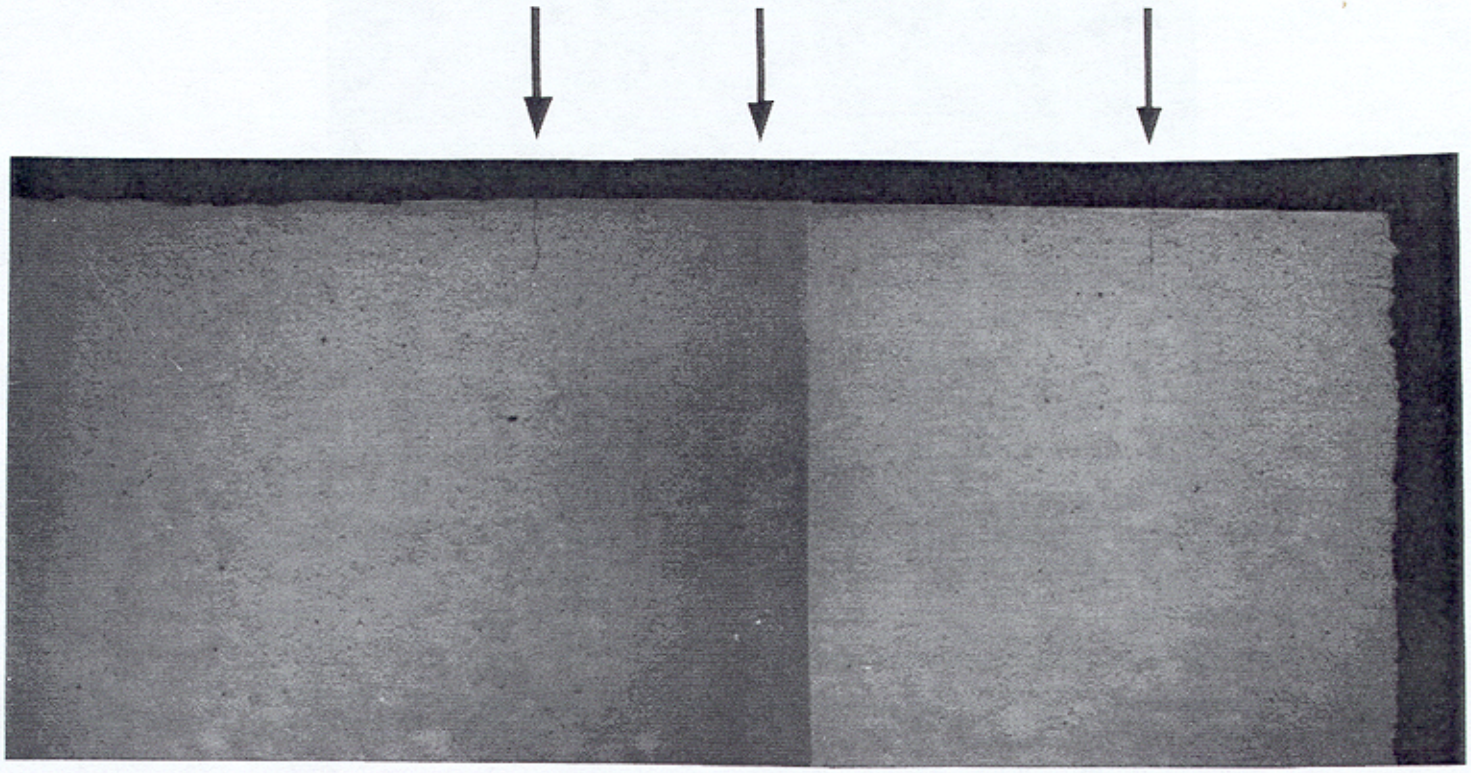

Figure 5. Montage of the Fracture Origin in the As-polished Condition. (Note the three additional grinding cracks [denoted by arrows] running parallel to the fracture plane; magnification 100x.)

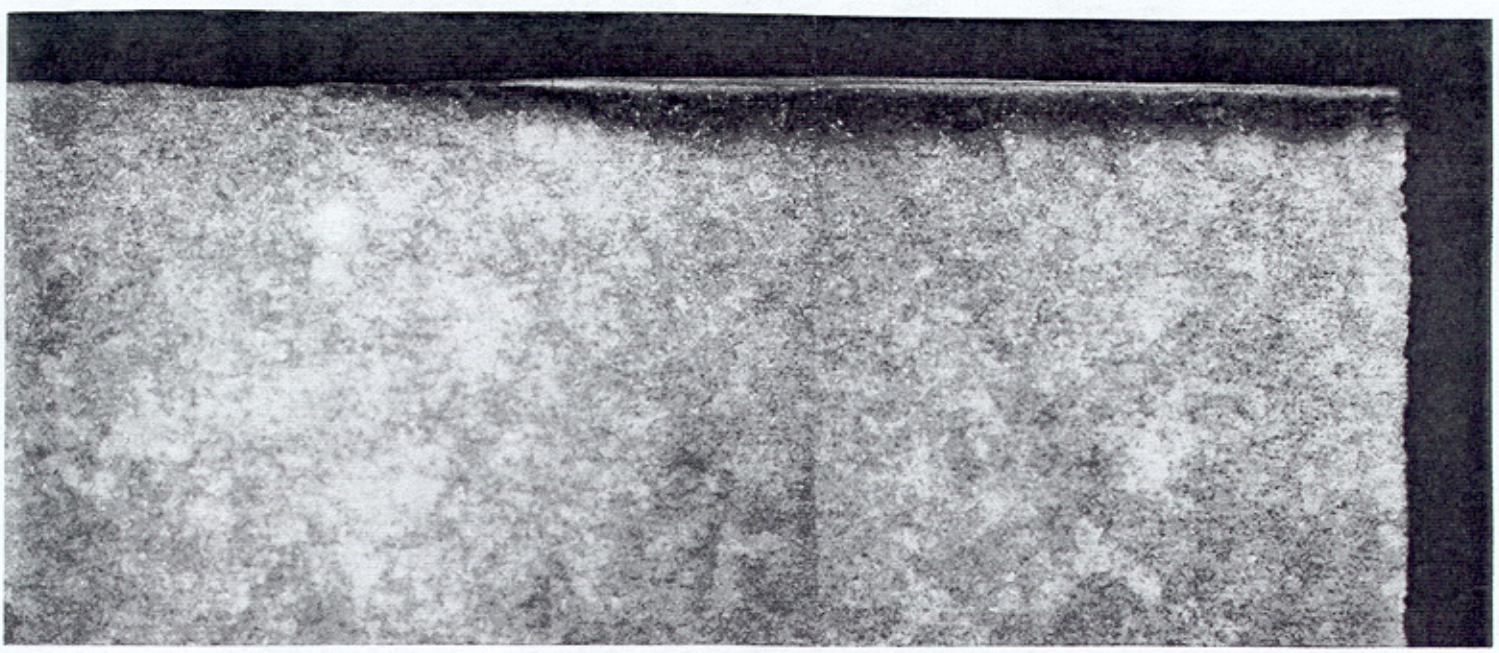

Figure 6. Montage of the Fracture Origin Shown in Figure 5, After Application of Vilella's Reagent. (Note that each crack is contained within the grinding burn; magnification 100x.)

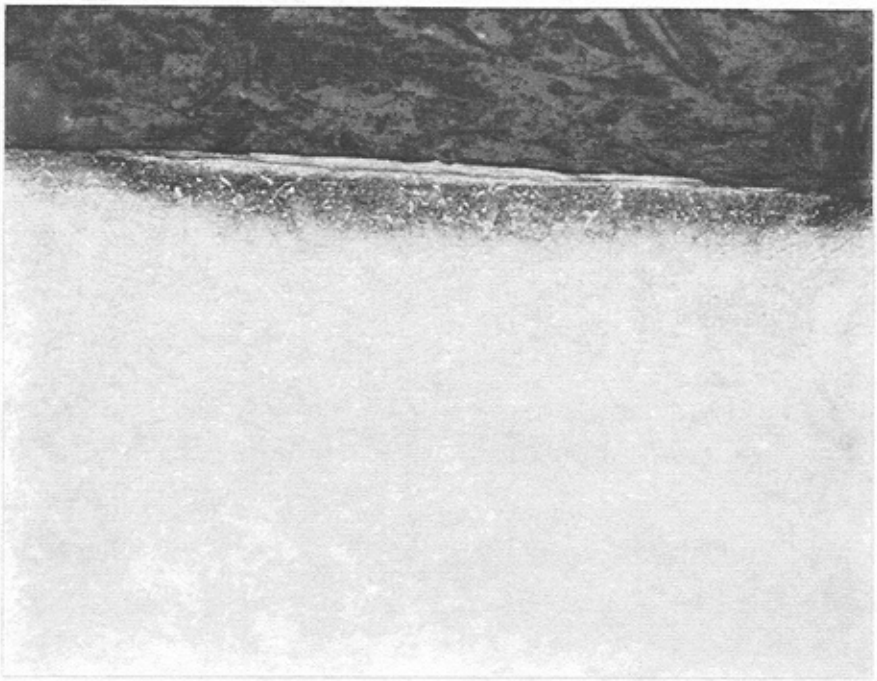

Figure 7. An Additional Grinding Burn Revealed Adjacent to the Fracture Origin, 0.43 Inch Away. (Note the white rehardened layer and the dark retempered layer; Vilella's reagent; magnification 150x.)

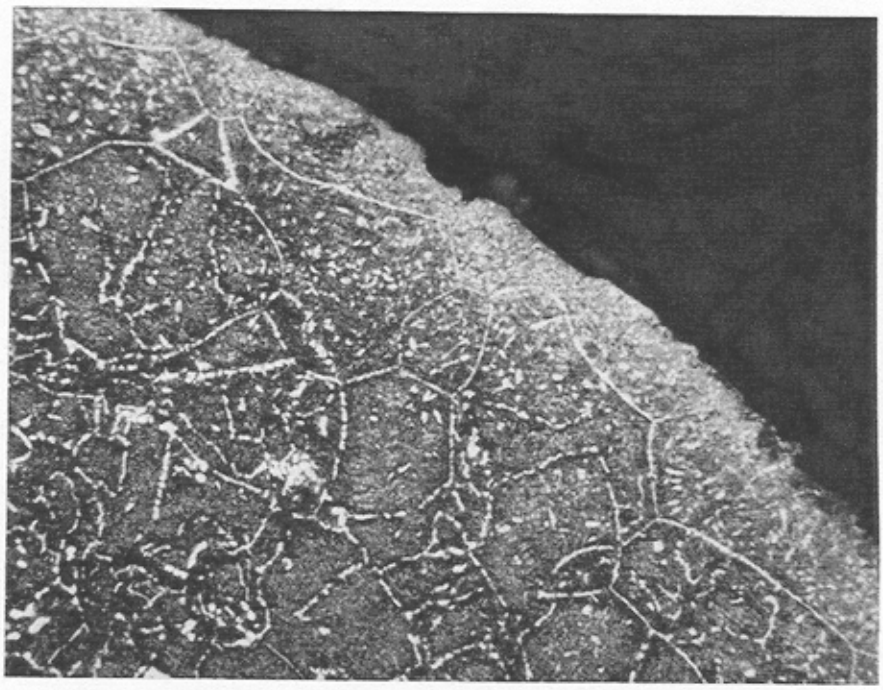

Figure 8. Metallographic Cross Section Through the Damping Ring Groove Region That was Double Carburized Inadvertently. (Note the carbide networks in the carburized case formed by this excess carbon; Villela's reagent; magnification 400x.)

Representative damping ring and gear tooth metallographic samples were analyzed to determine the extent of carbide formation with respect to part geometry. Figures 9 and 10 highlight the areas examined for this investigation. Figures 11 through 14 show Areas 1 through 4, respectively, on the gear tooth sample. Note that carbide formation was heavier in Areas 1 and 2 (the locations with more surface area exposed to the carburization atmosphere). No carbide networks were noted in the areas of high stress (Areas 3 and 4). Figures 15 through 18 show Areas 1 through 4, respectively, of the damping ring groove sample. Note the heavy carbide formation in Area 4, with respect to Areas 1 through 3. The structure had the appearance of CCNs, which are unacceptable per Boeing Specification D210-10342-1 [3]. Also note that Area 4 is the point where the catastrophic failure originated.

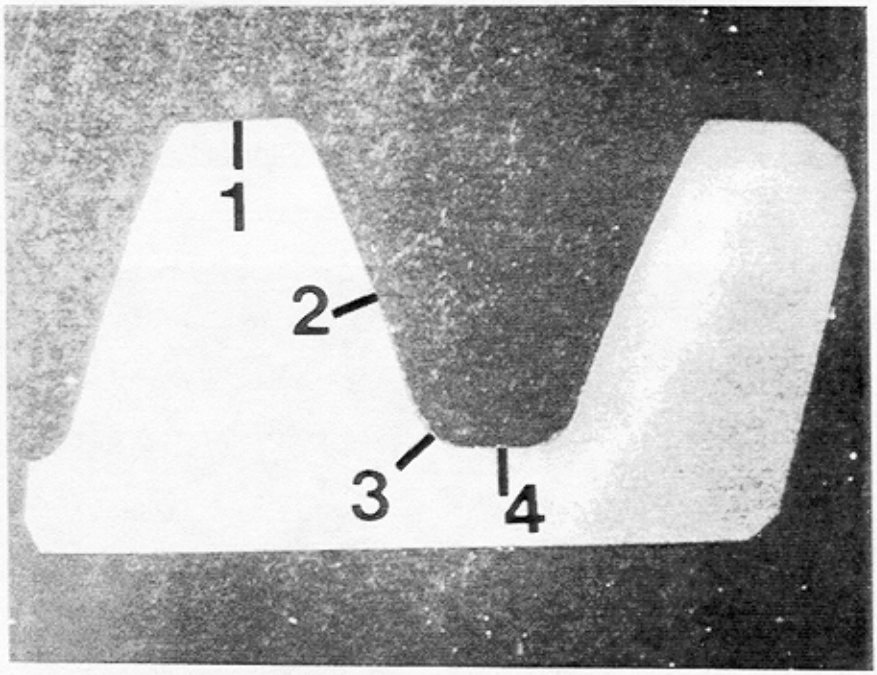

Figure 9. Macrograph of a Gear Tooth Sample Showing the Areas in Which the Carburized Case was Examined for Evidence of Carbide Networks (Vilella's reagent; magnification 8x).

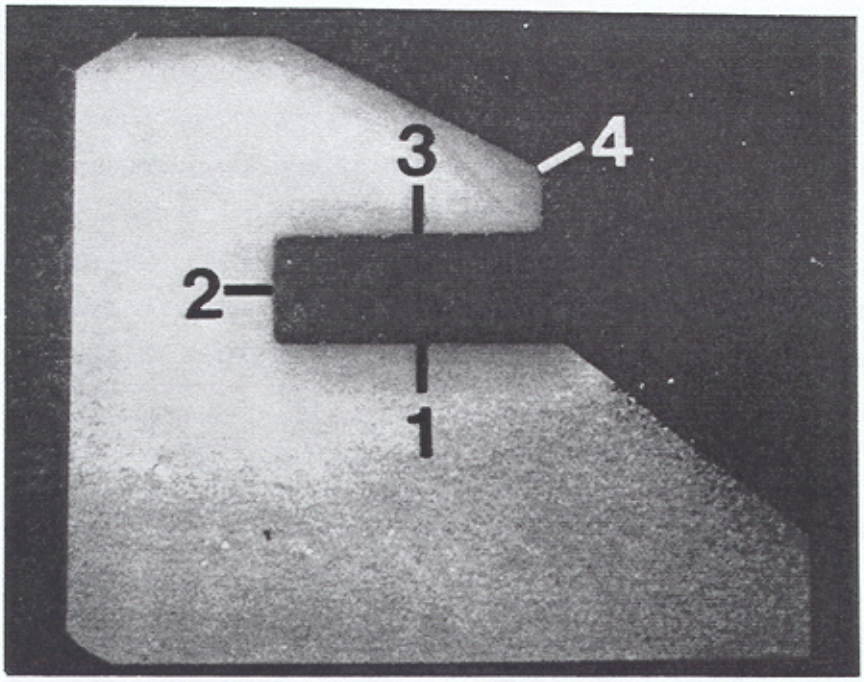

Figure 10. Macrograph of a Damping Ring Groove Sample Showing the Areas in Which the Carburized Case was Examined for Evidence of Carbide Networks (Vilella's reagent; magnification 8x).

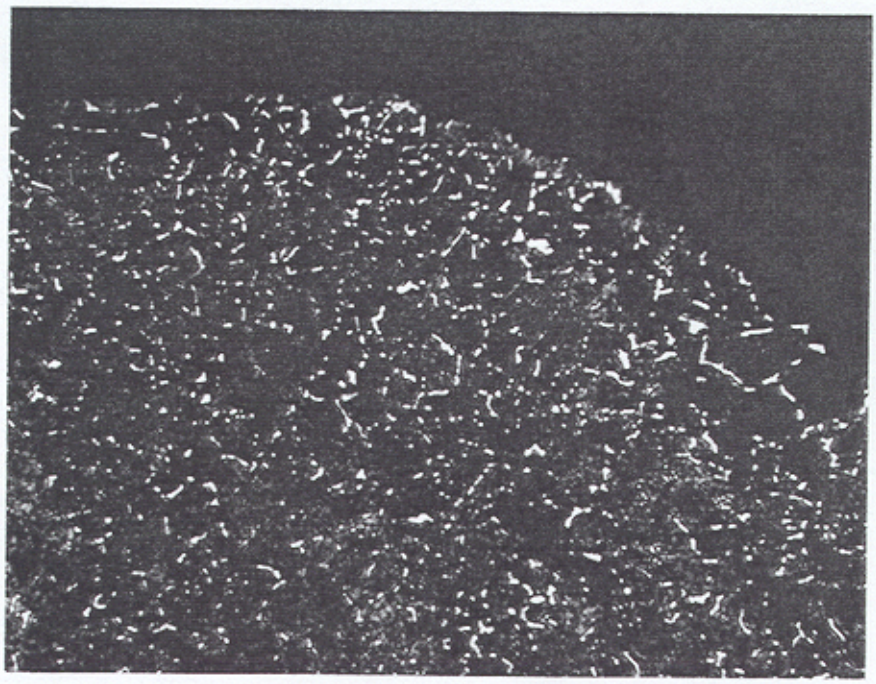

Figure 11. Micrograph of the Gear Tooth Metallographic Sample Showing the Case Microstructure Within Area 1 (Vilella's reagent; magnification 400x).

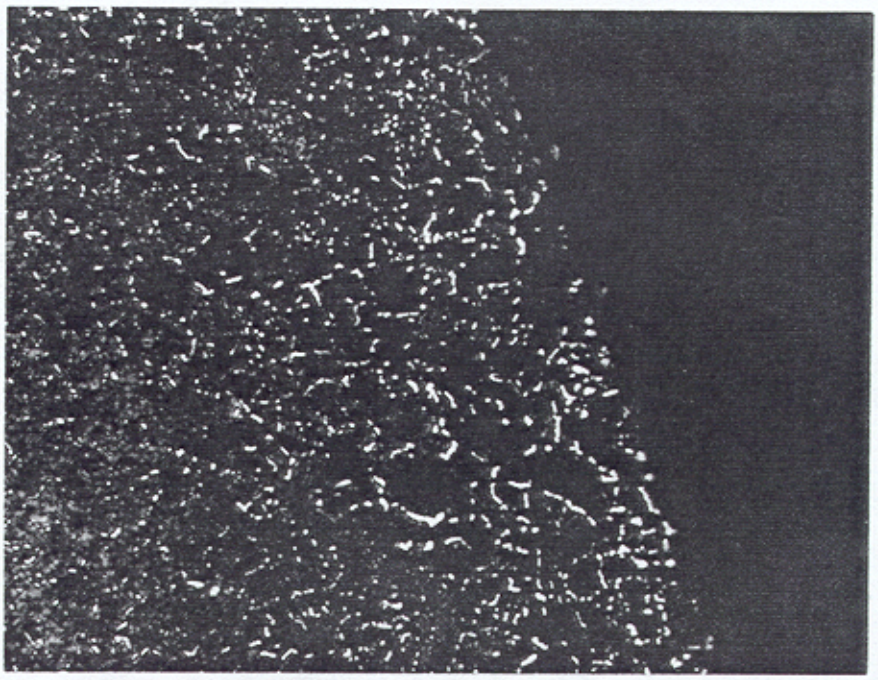

Figure 12. Micrograph of the Gear Tooth Metallographic Sample Showing the Case Microstructure Within Area 2 (Vilella's reagent; magnification 400x).

Figure 13. Micrograph of the Gear Tooth Metallographic Sample Showing the Case Microstructure Within Area 3 (Vilella's reagent; magnification 400x).

Figure 14. Micrograph of the Gear Tooth Metallographic Sample Showing the Case Microstructure Within Area 4 (Vilella's reagent; magnification 400x).

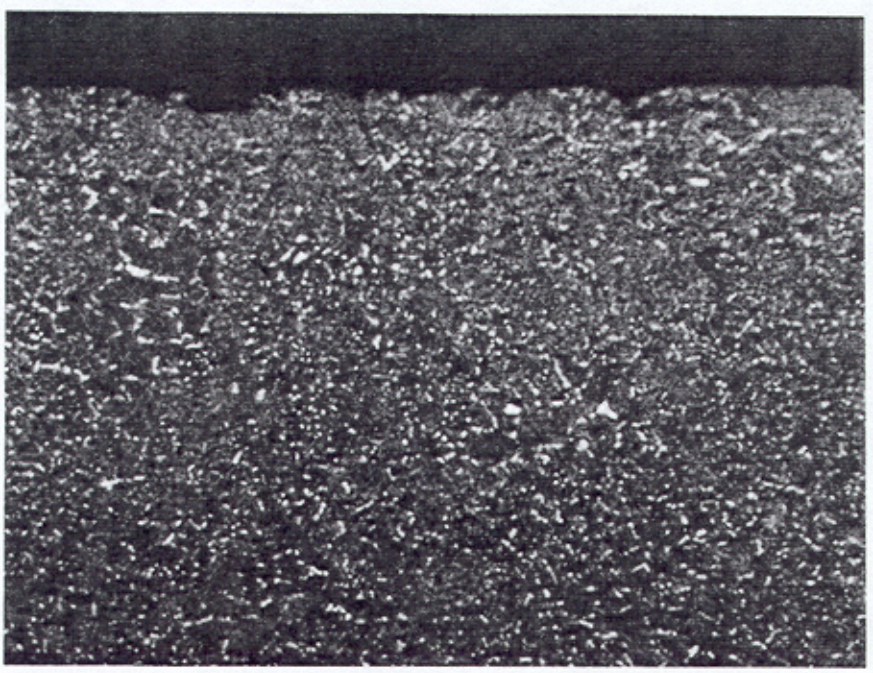

Figure 15. Micrograph of the Damping Ring Groove Metallographic Sample Showing the Case Microstructure Within Area 1 (Vilella's reagent; magnification 400x).

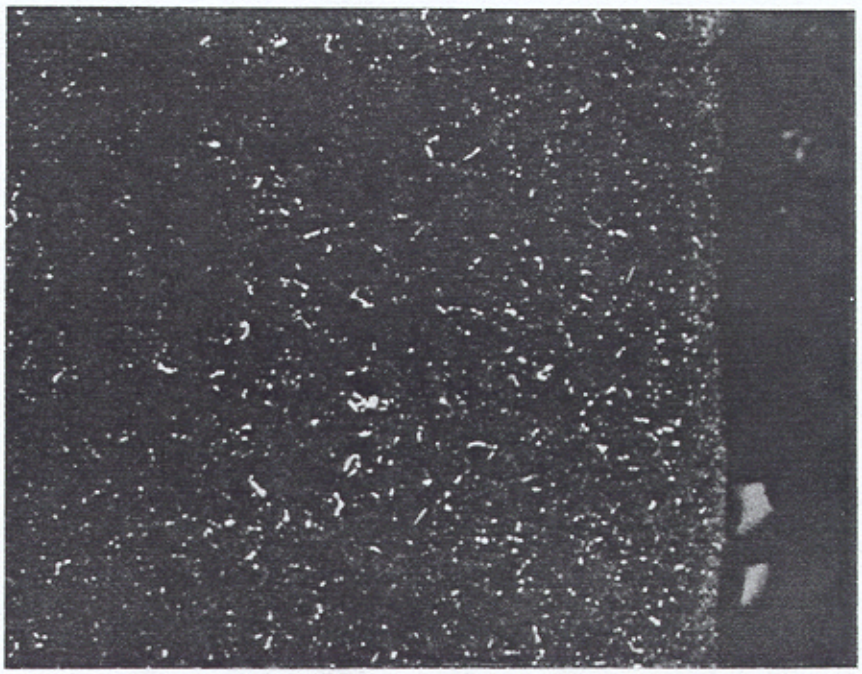

Figure 16. Micrograph of the Damping Ring Groove Metallographic Sample Showing the Case Microstructure Within Area 2 (Vilella's reagent; magnification 400x).

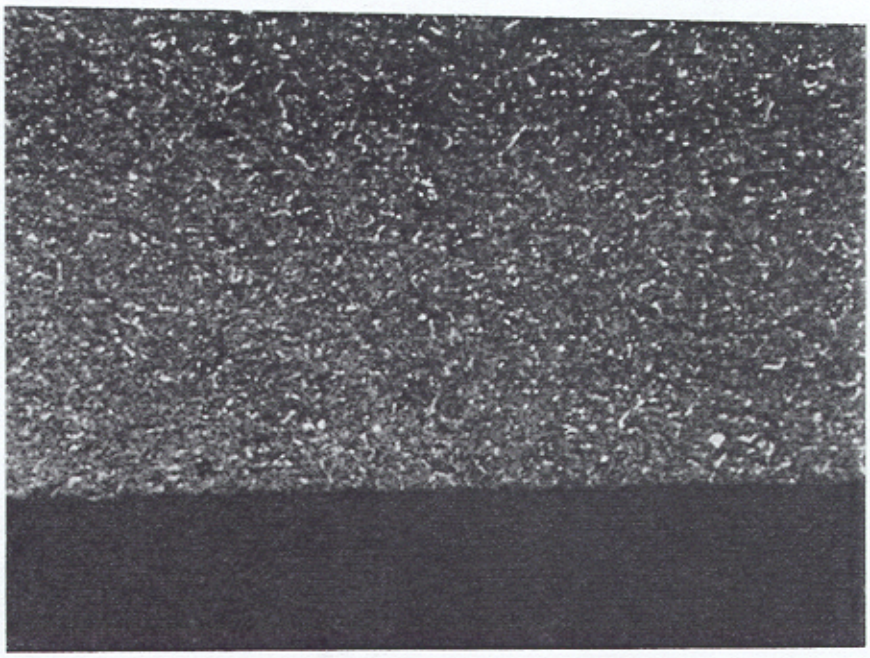

Figure 17. Micrograph of the Damping Ring Groove Metallographic Sample Showing the Case Microstructure Within Area 3 (Vilella's reagent; magnification 400x).

Figure 18. Micrograph of the Damping Ring Groove Metallographic Sample Showing the Case Microstructure Within Area 4 (Vilella's reagent; magnification 400x).

Metallography combined with microhardness testing of the damping ring groove area (fracture origin location) revealed a greater case depth than specified (see Hardness/Case Depth Measurement section for results). The core structure (see Figure 19) was consistent with the prior treatment (duplex structure of free ferrite within tempered martensite).

ARL examined a metallographic mount of spiral bevel gear P216, which Boeing had inadvertently included with the P196 gear parts when shipped to ARL. This sample was prepared and etched with Vilella's reagent by Boeing and exhibited the intergranular grinding crack shown in Figure 20. Although this part was not from the failed gear being investigated, and grinding cracks in this material have been known to travel in either an intergranular or transgranular direction, it served as an example of a grinding crack in X-2M steel following the path of a carbide network.

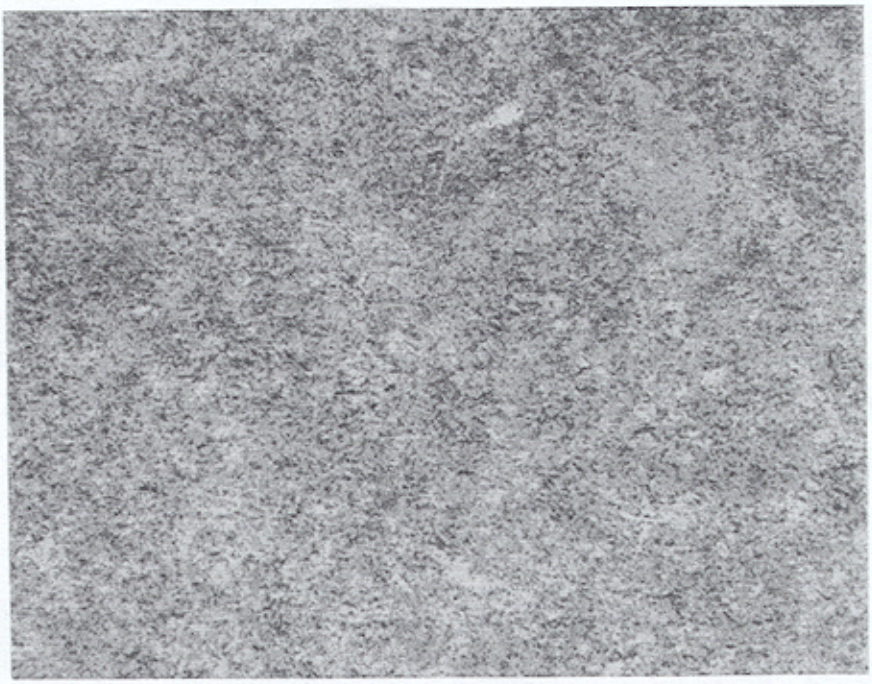

Figure 19. Micrograph of the Core Microstructure of the X-2M Steel Part. (The structure is consistent with the prior treatment; Vilella's reagent; magnification 200x.)

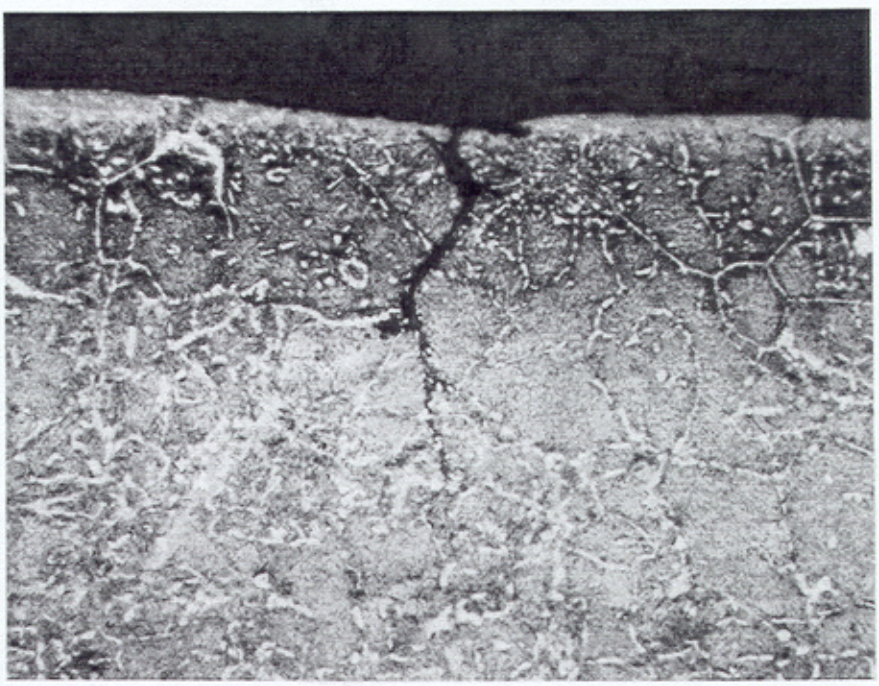

Figure 20. Micrograph of an Intergranular Crack Propagating Along a Carbide Network Noted in Gear P216. (This was not the failed gear being investigated, but this sample provided an example of a grinding crack following the path of a carbide network in X-2M steel; Vilella's reagent; magnification 400x.)

6. HARDNESS/CASE DEPTH MEASUREMENT

The case hardness was measured directly from a section of the component. A gear tooth portion was sectioned so that the tooth crest and base were parallel to validate hardness testing. The hardness was measured using the superficial Rockwell 15N scale, since the lighter major load (15 kg) posed less of a risk of penetrating the case depth compared to the major load of the Rockwell "C" scale (150 kg). The depths of the HR15N hardness indentation were calculated to ensure the 15-kg load did not penetrate the case and measure a composite of both the case and the core. The depth of penetration of the HR15N diamond indenter was calculated from the following formula [5]:

$$(100\text{-HR15N}) \times 0.001\text{mm} = \text{depth of penetration}$$

Applying this formula, a hardness of 88.9 HR15N (the lowest reading measured) had a depth of penetration of 0.00044 inch, which was safely within the required case depth of 0.030 to 0.050 inch. The readings were subsequently converted to the Rockwell "C" scale using standard conversion tables. Table 2 lists the results of case hardness testing. The average converted HRC measurement (61 HRC) conformed to the governing requirement of 59-64 HRC.

Table 2

Case Hardness Measurements
HR15N Scale
Major Load 15 kg

Reading	HR15N	Eq. HRC
1	90.0	60
2	88.9	57
3	90.1	60
4	91.0	62
5	90.1	60
6	90.6	61
7	91.1	62
8	92.4	66
9	91.5	63
10	90.3	60
Average	90.6 HR 15N	61 Required 59-64 HRC

The core hardness was measured using the Rockwell "C" scale. A total of four sections were analyzed. The results are listed in Table 3. Each reading conformed to the governing requirement of 36-44 HRC.

Table 3

Core Hardness Measurements
HRC Scale
Major Load 150 kg

Reading	Section 1	Section 2	Section 3	Section 4	
1	38.7	38.7	40.4	39.6	
2	38.7	39.2	40.5	40.4	
3	38.8	40.6	40.2	40.5	
4	38.6	40.2	40.7	40.2	
5	38.3	39.8	41.0	40.5	
6	39.7	40.3	40.7	40.7	
Average	38.8	39.8	40.6	40.3	Required 36-44 HRC

The effective case depth was measured from four metallographically prepared samples. Three samples represented gear tooth roots, and one sample represented the damping ring groove region. The case depth was defined as the perpendicular distance from the surface to a point where the microhardness of the part was 513 Vickers hardness number (VHN) (approximately 50 HRC)[1]. The case depths were measured directly from photomicrographs taken at 50x magnification. Table 4 contains the results of case depth measurements. Each root measurement met the governing requirement. However, a case depth of 0.075 inch was measured from the damping ring groove sample, which exceeded the maximum allowable case depth. It was later learned that the masking was inadvertently omitted before the second carburization cycle by the subcontractor contributing to this excessive case depth.

[1]Specification D210-10342-1 states that either a VHN of 653 (~HRC 58) or a VHN of 513 (~HRC 50) should be used to determine the effective case depth, based upon the drawing. The drawing states that the case hardness is required to be 59-64 HRC. However, the 513 VHN was used in this study to determine the effective case depth, based upon conversation with Boeing and industry practice.

Table 4

Case Depth Measurements
Vickers Microhardness Scale
500-gram load

Sample	Region	Case Depth (inch)
1	Root	0.053
2	Root	0.049
3	Root	0.044
4	Damping Ring	0.075
	Requirement	0.035-0.055 inch

7. X-RAY DIFFRACTION

X-ray diffraction was used by ARL to determine the amount of retained austenite within the structure of the failed part. A Technology for Energy Corporation (TEC) stress analyzer was used, with data collected using CrKa radiation. A voltage of 45 kV and a beam current of 1.75 mA were used. The data were analyzed using the parafocusing technique. Specification D210-10342-1 states that the maximum allowable amount of retained austenite shall be 20%. Two samples were analyzed, and results of 8.81% and 8.94% retained austenite were obtained. These values conformed to the governing specification.

8. SCANNING ELECTRON MICROSCOPY/ENERGY-DISPERSIVE SPECTROSCOPY

The length of fatigue crack propagation on the fractured part was approximately 1.65 inch, followed by a ductile overload region. The fracture origin was located at a defect within the damping ring groove region. The defect was "half moon" shaped and had a depth of approximately 0.005 inch and a length of approximately 0.015 inch. The defect contained a darkened film, which was considered evidence of a pre-existing crack opened to the surface during the black oxide treatment. Figure 21 shows a micrograph displaying the featureless origin in the backscatter mode. Figures 22 and 23 show a representative fatigue and overload morphology, respectively. The fatigue region was characterized by a transgranular morphology, while the overload region contained ductile dimples as the result of microvoid coalescence. Approximately

0.08 inch away from the origin along the 30° tapered surface, an intergranular morphology was noted, as shown in Figure 24. This was the region that displayed CCNs during metallographic examination, and it is believed the grinding crack responsible for this failure propagated along these networks.

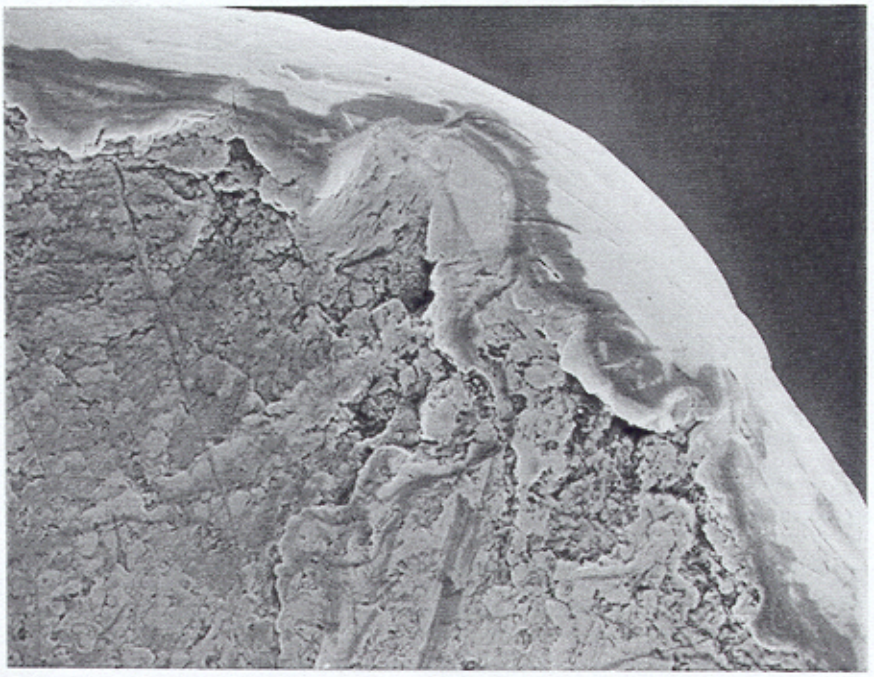

Figure 21. Scanning Electron Micrograph of the Fracture Origin. (Note the featureless morphology, common with fatigue fractures; magnification 350x.)

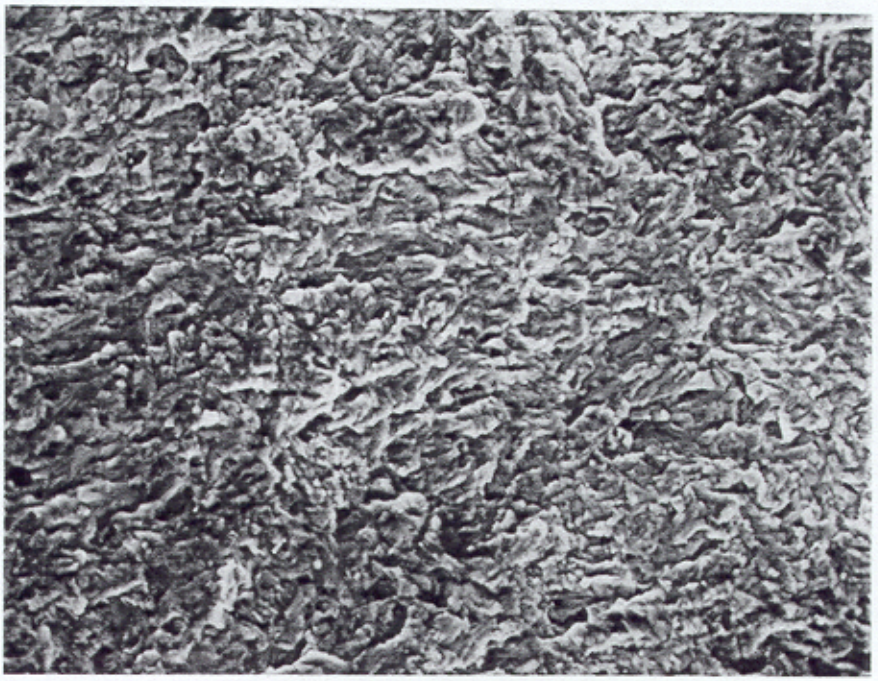

Figure 22. Scanning Electron Micrograph of the Fatigue Morphology, Predominant on the Primary Fracture Surface (magnification 1000x).

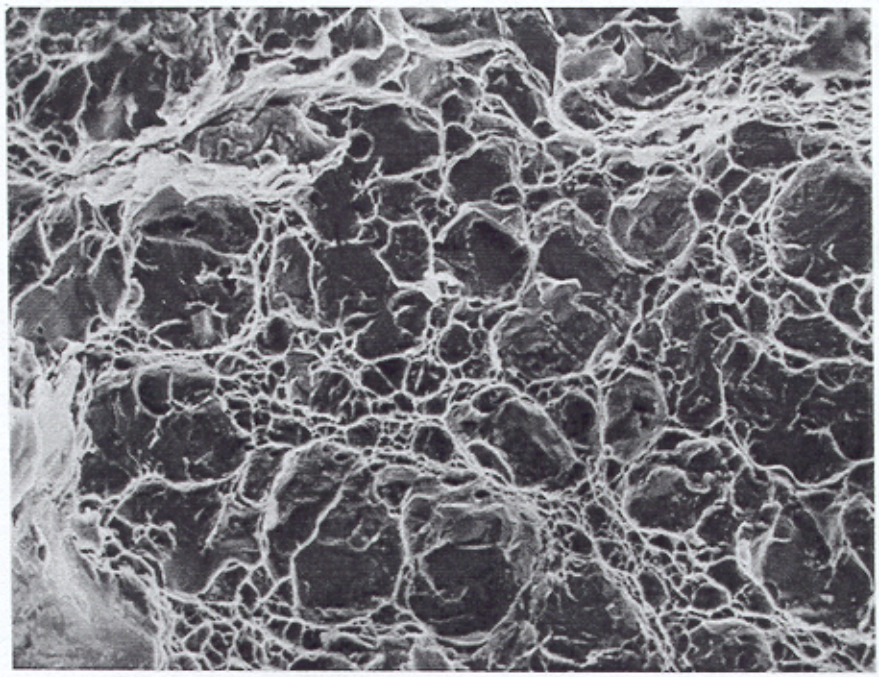

Figure 23. Scanning Electron Micrograph of the Overload Morphology, Noted on the Remaining Primary Fracture Surface (magnification 500x).

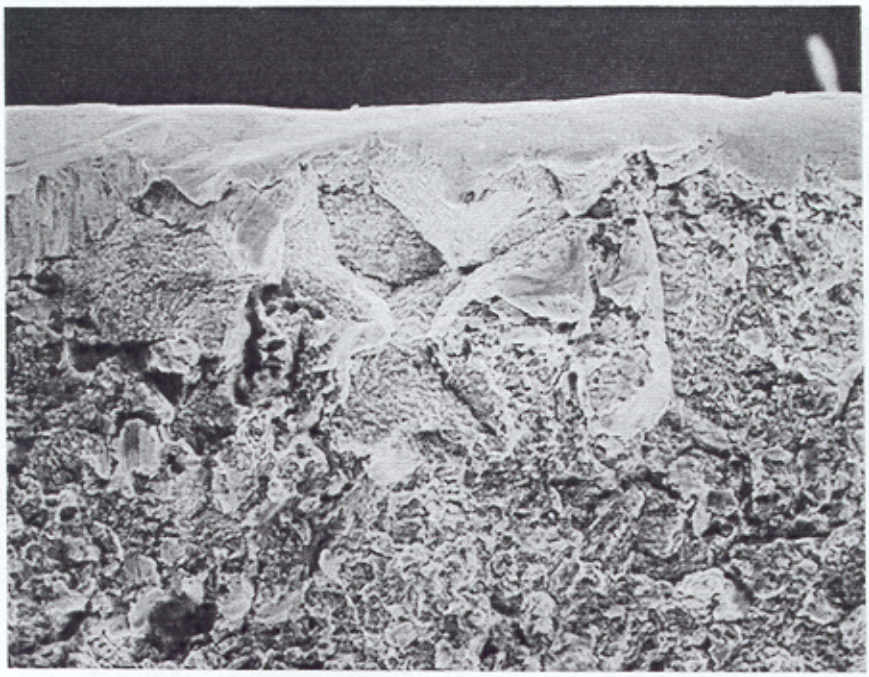

Figure 24. Scanning Electron Micrograph of the Intergranular Morphology Noted Within the Carburized Case, Noted 0.08 Inch Away From the Primary Fracture Origin (magnification 400x).

ARL confirmed Boeing's finding by using energy-dispersive spectroscopy to reveal the presence of sodium within the defect. This was evidence that the crack was open to the surface during the black oxide finish process. Sodium nitrate and sodium dichromate are two chemicals typically used in the black oxide process, which would account for the presence of sodium. Spectra obtained outside the darkened area contained no evidence of sodium.

Further evidence of intergranular cracking was observed on a secondary fracture surface. The fracture was a section of the damping ring groove region (away from the origin), as the chamfer between the 30° taper and the 7.125-inch diameter was clearly recognizable. Fractographic examination of this "through crack" revealed an intergranular morphology within the carburized case, in a region similar to that of the fracture origin. Figure 25 shows a portion of the piece examined at low magnification, while Figure 26 shows the intergranular region within the carburized case of the part. Figure 27 shows the grains at higher magnification. Traversing toward the core of the specimen, a transgranular morphology consistent with fatigue in X-2M steel was evident (see Figure 28). Within the center of the specimen, an overload morphology (as shown in Figure 29) was predominant. The intergranular zone measured approximately 0.001 inch deep. The fatigue zone measured 0.008 inch into the core from the end of the intergranular region, and the overload zone measured 0.012 inch deep from the fatigue zone. This finding was evidence that a grinding crack had propagated along the CCNs within the case of the carburized component, then propagated by fatigue until final fast fracture.

Figure 25. Scanning Electron Micrograph of a Portion of a Secondary Fracture Surface. (This fracture occurred in the damping ring groove region, most likely from a grinding crack. The fracture surface contained an intergranular morphology within the carburized case, followed by a fatigue zone, and finally an overload region toward the center of the piece; magnification 20x.)

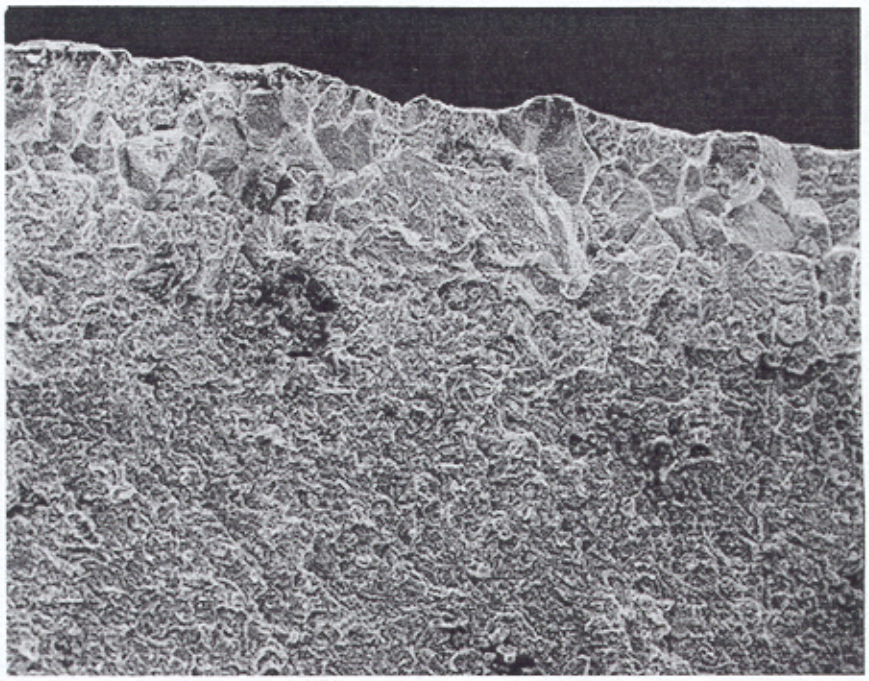

Figure 26. Scanning Electron Micrograph Showing the Intergranular Morphology Within the Carburized Case of the Secondary Fracture (magnification 200x).

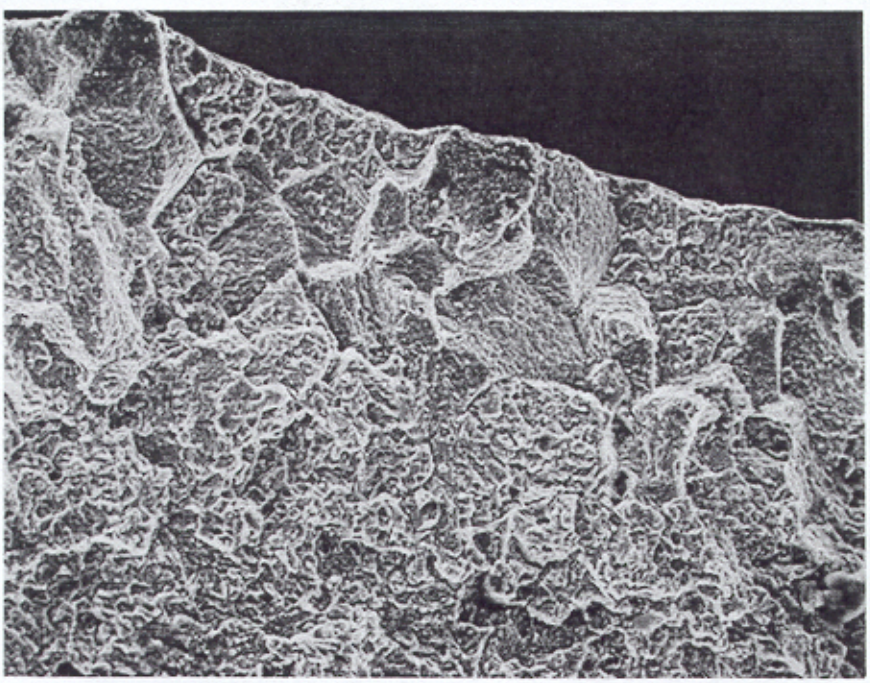

Figure 27. Scanning Electron Micrograph Showing the Intergranular Morphology of Figure 26 at Higher Magnification (magnification 400x).

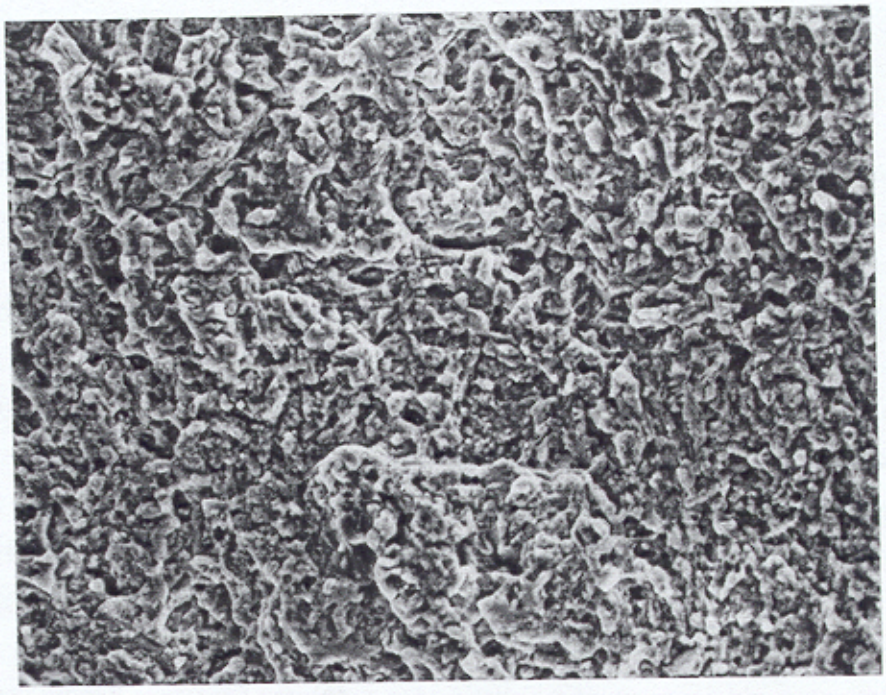

Figure 28. Scanning Electron Micrograph Showing a Morphology Consistent With the Fatigue Region Noted Within the Primary Fracture (see Figure 22). (This region was located between the intergranular and overload zones; magnification 1000x.)

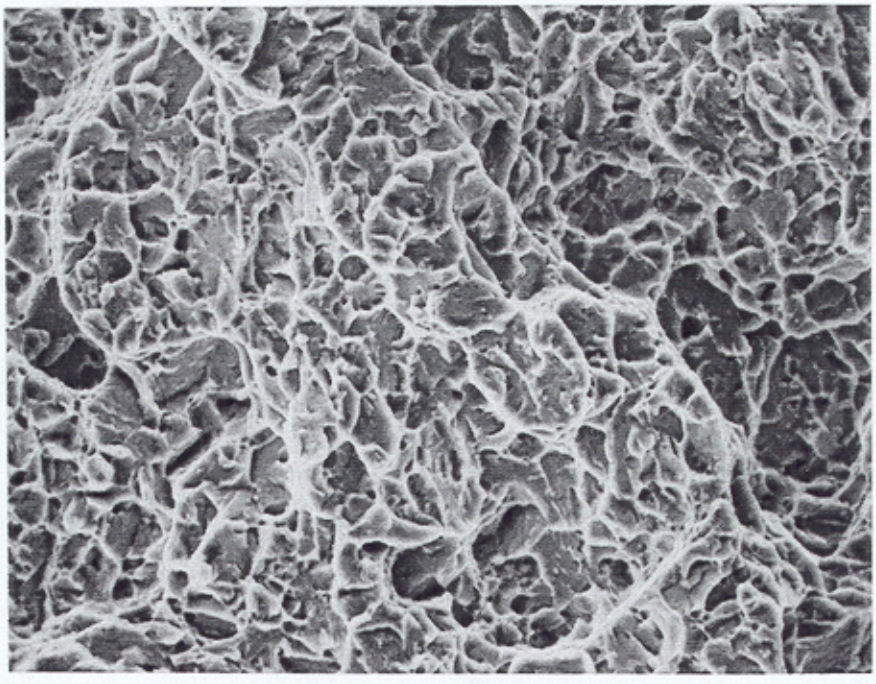

Figure 29. Scanning Electron Micrograph Showing the Overload Morphology Noted at the Center of the Failed Piece (magnification 1000x).

9. DISCUSSION

9.1 CCNs

Carbide networks form in austenitic grain boundaries when parts are carburized at an elevated temperature and then slowly cooled. Carbon is rejected to these grain boundaries as the solubility limit is exceeded during cooling. It is well documented (for steels in general) that continuous carbide networks tend to embrittle the case and are usually avoided [5]. The Carburizing and Carbonitriding Handbook by the American Society for Metals (ASM) [6] shows a set of micrographs of American Institute for Steel and Iron (AISI) 9310 steel, detailing the acceptable and unacceptable characteristics of each. Micrographs similar to the structure of the gear being investigated were labeled unacceptable because of the presence of excessive carbides, some of which formed continuous networks along grain boundaries. Higgins states, "If the carbon content of the case is higher than 0.8% (the eutectoid composition) a network of primary cementite will coincide with the grain-boundary sites of the original austenite giving rise to intercrystalline brittleness and consequent exfoliation (or peeling) of the case during service." [7]. The handbook by ASM entitled "Case Hardening of Steel" states, "For most parts, (gears, for example), excess carbide in the grain boundaries is considered undesirable." [8]. Also, the ASM handbook entitled "Systematic Analysis of Gear Failures" states, "Massive carbides may be acceptable in some instances, but if a network appears, it is most unwelcome." [9].

A joint effort was undertaken by the Army and Boeing from 1982 to 1990 to optimize a high temperature vacuum carburizing procedure for AISI 9310 gear steel and X-2M steel (Contract No. DAAG46-82-C-0034). This process would significantly reduce the processing time for gears, and ultimately lower the cost. The program was successful for AISI 9310, but not for X-2M. The process was not optimized for the X-2M steel primarily because of the presence of CCNs upon carburizing. As a result of this program, a contractor technical report (Materials Technology Lab [MTL] TR 90-42) was written entitled, "Aircraft Quality High Temperature Vacuum Carburizing" [10]. This report states that "CCNs are an undesirable condition for good bending fatigue resistance" and "refinements to the vacuum carburizing technique for X-2M were undertaken to eliminate this type of unwanted structure." This report contains a micrograph of an unacceptable X-2M case microstructure (shown in Figure 30). This structure is quite similar to that of the double carburized 30 degree taper sample from the damping ring groove region (compare to Figure 8).

The Boeing specification for AISI 9310 steel contains a figure that displays micrographs of acceptable and unacceptable case structures with respect to CCNs. However, the Boeing

specification for X-2M steel (which forms carbides more readily than AISI 9310) contains only the statement, "The presence of a continuous intergranular carbide network at the surface is unacceptable." No micrographs are included in this specification to distinguish acceptable structures from unacceptable structures.

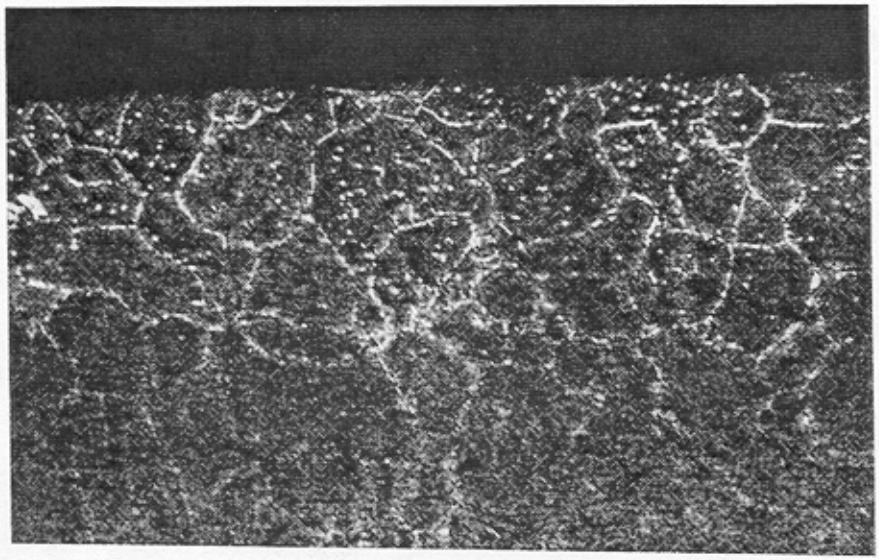

Figure 30. A Micrograph Taken From Boeing's Technical Report, "Aircraft Quality High Temperature Vacuum Carburizing." (This structure was deemed unacceptable because of CCNs. Compare this structure to that of the failed component [see Figure 8], taken within the double carburized 30° taper region; magnification 400x.)

9.2 The Effect of CCNs on Material Properties

Very little information exists in open literature with respect to the effects of carbide networks on X-2M material properties. With respect to general comments about this structure, ASM's Handbook on Failure Analysis states, "Fatigue resistance of a component may be increased by case carburizing, provided the treatment is carried out properly so as to avoid gross structural discontinuities, such as carbide networks." [11]. In addition, Parrish states that "under bending fatigue conditions continuous networks appear to reduce the fatigue limit" and adds that, "when failure eventually occurs, it does so down the carbide network." [12]. Summarizing, Parrish notes that "carburized cases containing free carbides are relatively weak in response to static bending and impact bending." Statements such as these and those previously referenced are assumed to pertain to all carburizing grade steels.

9.3 CCNs and Grinding

Grinding is required to be performed on these gears before subsequent stress relieving and shot peening. However, conversation with Boeing and the Aviation and Troop Command (ATCOM) revealed that unauthorized re-work was performed on the subject gear, whereby grinding was performed after the stress relief and shot peening, for burr removal.

Grinding problems can occur if excess heat is generated at the part surface. Many factors contribute to grinding problems including worn grinding wheels, improper wheels, or removal of too much stock. Any of these scenarios can produce a tempering of the martensitic surface (dark layer), resulting in a reduced surface hardness, as well as a rehardening burn which produces a thin, hard layer of martensite (white layer) at the surface. These two anomalies were noted at the origin of this failure. The presence of CCNs within the case that contained the grinding burn aggravated the situation. Parrish states that "carbide networks can render a surface sensitive to grinding, the cracks tending to follow the path of the network." The grinding crack at the origin of the failure being investigated followed the path of the network as evidenced by the intergranular morphology along the 30° taper.

Although much is documented concerning the negative aspects of CCNs, their detrimental effects can be minimized by ensuring that no surface defects (such as grinding cracks/burns) exist on the surface of the component. Therefore, it is essential that nondestructive techniques used during the manufacturing sequence (i.e., magnetic particle inspection, 10x visual inspection, and nital etch inspection) are sensitive enough to reveal grinding cracks and burns.

10. CONCLUSIONS

Two extraordinary events occurred leading to the demise of gear P196: the part was unmasked in the damping ring groove and subjected to a double carburization, and grinding was performed as the final step, to provide dimensional tolerance. These events acted to produce excessive carbide formation in the damping ring groove region, as well as undetected grinding burns and cracks within the same area. This deleterious combination coexisted in service until a grinding crack propagated in fatigue to final fast fracture.

11. ACTION

As a result of this failure, added improvements have been incorporated into the manufacturing sequence to eliminate the occurrence of this type of defect in the future. First, an additional magnetic particle inspection has been added to the manufacturing sequence, as well as

an additional 10x visual inspection. Also, the grinding process that previously produced the damping ring groove has been replaced with a less detrimental turning process. In addition, a process has been developed as a guideline for burr removal in this region (previously, no process existed). Finally, the contractor has agreed to consider an addition to the X-2M material specification which would include reference micrographs of unacceptable case microstructures.

INTENTIONALLY LEFT BLANK

REFERENCES

[1] Doran, J., Walsh, R., and Cunningham, R., Boeing Materials Engineering Laboratory Report No. 93-105, dated 15 December 1993.

[2] Fopiano, P., Oliver, S., and Kula, E., "The Effect of Heat Treatment on the Structure and Properties of Standard and Modified Vasco X-2M Steel, AMMRC TR 77-8, March 1977.

[3] Boeing Specification D210-10342-1, "Carburizing and Hardening of BMS 7-223 Steel Components for Helicopters," REV LTR B, 1977.

[4] American Society for Metals (ASM) Handbook, Volume 8, Mechanical Testing, "Rockwell Hardness Testing," 1992.

[5] American Society for Metals (ASM) Handbook, Volume 18 , Friction, Lubrication and Wear Technology, "Carburizing," 1992.

[6] American Society for Metals (ASM) Reference Book, "Carburizing and Carbonitriding," 1977.

[7] R.A. Higgins, "Engineering Metallurgy, Applied Physical Metallurgy," 1988.

[8] American Society for Metals (ASM) Handbook, "Case Hardening of Steel," 1990.

[9] American Society for Metals (ASM) Handbook, "Systematic Analysis of Gear Failures," 1985.

[10] Cunningham, R.J. and Drago, R.J., "Aircraft Quality High Temperature Vacuum Carburizing," MTL TR 90-42, November, 1990.

[11] American Society for Metals (ASM) Handbook, Volume 11 , Failure Analysis and Prevention, "Fatigue Failures," 1985.

[12] Parrish, G., "The Influence of Microstructure on the Properties of Case-Carburized Components," 1990.

INTENTIONALLY LEFT BLANK

NO. OF COPIES	ORGANIZATION
2	ADMINISTRATOR DEFENSE TECHNICAL INFO CENTER ATTN DTIC DDA 8725 JOHN J KINGMAN RD STE 0944 FT BELVOIR VA 22060-6218
1	DIRECTOR US ARMY RESEARCH LABORATORY ATTN AMSRL CS AL TA RECORDS MANAGEMENT 2800 POWDER MILL RD ADELPHI MD 20783-1197
1	DIRECTOR US ARMY RESEARCH LABORATORY ATTN AMSRL CI LL TECHNICAL LIBRARY 2800 POWDER MILL RD ADELPHI MD 207830-1197
1	DIRECTOR US ARMY RESEARCH LABORATORY ATTN AMSRL CS AL TP TECH PUBLISHING BRANCH 2800 POWDER MILL RD ADELPHI MD 20783-1197
2	COMMANDER US ARMY MATERIEL COMMAND ATTN AMCSCI AMCQA P S J LORBER 5001 EISENHOWER AVENUE ALEXANDRIA VA 22333-0001
4	CDR HQ AMCCOM ATTN AMSMC PCA WM J WELLS AMSMC QAM I G SMITH AMSMC ASR M B KUNKEL J HOUSEMAN ROCK ISLAND IL 61299-6000
7	CDR US ARMY ATCOM ATTN AMSAV ECC E BUELTER R LAWYER AMSAV EFM F BARHORST K BHANSALI AMSAV E C SMITH AMCPM AAH D ROBY B KENNEDY ST LOUIS MO 63120-1798

NO. OF COPIES	ORGANIZATION
4	CDR CORPUS CHRISTI ARMY DEPOT ATTN AMSAV MRPD N HURTA L NERI MAIL STOP 55 SDSCC QLM D GARCIA C WILSON MAIL STOP 27 CORPUS CHRISTI TX 78419-6195
1	CDR US ARMY ARDEC ATTN SMCAR CCS C A SEBASTO BLDG 1 PICATINNY ARSENAL NJ 07806-5000
	ABERDEEN PROVING GROUND
2	DIRECTOR US ARMY RESEARCH LABORATORY ATTN AMSRL CI LP (TECH LIB) BLDG 305 APG AA
20	DIRECTOR US ARMY RESEARCH LABORATORY ATTN AMSRL WM MD (M PEPI) BLDG 4600

INTENTIONALLY LEFT BLANK

REPORT DOCUMENTATION PAGE

Form Approved OMB No. 0704-0188

1. AGENCY USE ONLY *(Leave blank)*	2. REPORT DATE	3. REPORT TYPE AND DATES COVERED
	August 1997	Final

4. TITLE AND SUBTITLE

Metallurgical Examination of Failed Spiral Bevel Gear P196, Part No. 145D6302

5. FUNDING NUMBERS

6. AUTHOR(S)

Pepi, M.S. (ARL)

7. PERFORMING ORGANIZATION NAME(S) AND ADDRESS(ES)

U.S. Army Research Laboratory
Weapons & Materials Research Directorate
Aberdeen Proving Ground, MD 21010-5066

8. PERFORMING ORGANIZATION REPORT NUMBER

9. SPONSORING/MONITORING AGENCY NAME(S) AND ADDRESS(ES)

U.S. Army Research Laboratory
Weapons & Materials Research Directorate
Aberdeen Proving Ground, MD 21010-5066

10. SPONSORING/MONITORING AGENCY REPORT NUMBER

ARL-TR-1432

11. SUPPLEMENTARY NOTES

12a. DISTRIBUTION/AVAILABILITY STATEMENT

Approved for public release; distribution is unlimited.

12b. DISTRIBUTION CODE

13. ABSTRACT *(Maximum 200 words)*

A failed spiral bevel gear was examined by the U.S. Army Research Laboratory (ARL), Weapons and Materials Research Directorate, Weapons Concepts Division (WM-MD) after the primary contractor (Boeing Helicopters Co.) performed the initial investigation. The gear was fabricated from X-2M steel. Light optical microscopy of the failed gear section revealed characteristics consistent with a fatigue failure. The fracture origin was characterized by a darkened, half-moon-shaped region. Energy-dispersive spectroscopy of the darkened region revealed the presence of sodium, evidence that the crack was open to the black oxide finish process. The pre-existing crack was oriented perpendicular to the direction of grinding, indicating the possibility of a grinding crack. Metallography confirmed that the pre-existing crack was a grinding burn, since evidence of rehardening and retempering was observed. Contributory to crack propagation was the presence of carbide networks within the carburized case. Metallographic examination, combined with microhardness testing, revealed a deeper than acceptable case in the damping ring groove region (origin location). It was later learned that this region was mistakenly subject to a double carburization during processing. Although the morphology of the origin was featureless, fractographic examination of a secondary fracture (most likely an additional grinding crack) did reveal an intergranular "rock candy" morphology. This was evidence that the crack propagated along the carbide network within the carburized case. It was concluded that the cracks had formed during the grinding process and had propagated along the carbide network until final fast fracture.

14. SUBJECT TERMS

carbide networks, carburization, failure analysis, fatigue, metallurgical examination, spiral bevel gear, X-2M steel

15. NUMBER OF PAGES

42

16. PRICE CODE

17. SECURITY CLASSIFICATION OF REPORT	18. SECURITY CLASSIFICATION OF THIS PAGE	19. SECURITY CLASSIFICATION OF ABSTRACT	20. LIMITATION OF ABSTRACT
Unclassified	Unclassified	Unclassified	